**Supplemental Material**

# Methane source attribution in a U.S. dry gas basin using spatial patterns of ground and airborne ethane and methane measurements

Ingrid Mielke-Maday[1,2*], Stefan Schwietzke[1,2], Tara I. Yacovitch[3], Benjamin Miller[1,2], Steve Conley[4], Jonathan Kofler[1,2], Philip Handley[1,2], Eryka Thorley[1], Scott C. Herndon[3], Bradley Hall[2], Ed Dlugokencky[2], Patricia Lang[2], Sonja Wolter[1,2], Eric Moglia[1,2], Molly Crotwell[1,2], Andrew Crotwell[1,2], Michael Rhodes[1,2], Duane Kitzis[1,2], Timothy Vaughn[5], Clay Bell[5], Dan Zimmerle[5], Russ Schnell[2], and Gabrielle Pétron[1,2].

[1] Cooperative Institute for Research in Environmental Sciences, University of Colorado Boulder, Boulder, Colorado, USA

[2] NOAA Earth System Research Laboratory, Boulder, Colorado, USA

[3] Aerodyne Research, Inc., Billerica, Massachusetts, USA

[4] Department of Land, Air, and Water Resources, University of California Davis, Davis, California, USA

[5] Energy Institute and Department of Mechanical Engineering, Colorado State University, Fort Collins, Colorado USA

* corresponding author. Ingrid.mielkemaday@colorado.edu

**Contents**

## Section 1. Mobile laboratory calibration protocol

Calibration standards were prepared in aluminum cylinders using whole air spiked with methane ($CH_4$) and ethane ($C_2H_6$). Prior to and following field deployment, calibration standards were measured in the National Oceanic and Atmospheric Administration (NOAA) Earth System Research Laboratory (ESRL) Global Monitoring Division (GMD) laboratory in Boulder, CO, yielding the values listed in Table S1. One cylinder was depleted during the campaign and therefore could not be reanalyzed after the campaign. Calibration cylinders were measured for $CH_4$ immediately upon return from the field and were measured for $C_2H_6$ six months following field deployment.

**Table S1: ML field calibration tank values.** $CH_4$ and $C_2H_6$ values of calibration tanks measured in the NOAA GMD laboratory prior to and following field deployment.

| Calibration cylinder serial number | Preparation date | Pre-campaign calibrated $CH_4$ | Post-campaign calibrated $CH_4$ | Pre-campaign calibrated $C_2H_6$ | Post-campaign calibrated $C_2H_6$ |
|---|---|---|---|---|---|
| FF17696 | March 1, 2015 | 1893.59 ppb | 1893.84 ppb | 2.035 ppb | 2.036 ppb |
| FF17646 | March 1, 2015 | 1862.71 ppb | N/A | 10.53 ppb | N/A |
| FF17726 | March 1, 2015 | 2200.03 ppb | 2199.76 ppb | 19.89 ppb | 20.20 ppb |

Calibrations of the TILDAS were used primarily to monitor instrument performance and diagnose problems. NOAA GMD laboratory measurements by GC-MS of $C_2H_6$ and $CH_4$ in the calibration cylinders are on the NOAA 2016 and WMO X2004A scales, respectively. NOAA GMD is the World Meteorological Organization, Global Atmosphere Watch Central Calibration Laboratory for $CH_4$.

Measurements of the cylinders from the TILDAS analyzer are plotted against laboratory-measured values to create twice daily calibration curves, which yield consistent slopes for each calibration, but inconsistent y-intercepts. So, the reciprocal of the slope is applied as a calibration factor to both $CH_4$ and $C_2H_6$ gradients (1.04 and 1.05, respectively) and these corrected values are used to calculate ERs. $CH_4$ and $C_2H_6$ TILDAS absolute mixing ratios are therefore not externally calibrated. The $C_2H_6$ slope of 0.95 is consistent with the 0.94 determined by Yacovitch et al. (2014) for another Aerodyne $C_2H_6$ TILDAS (2997 $cm^{-1}$ laser).

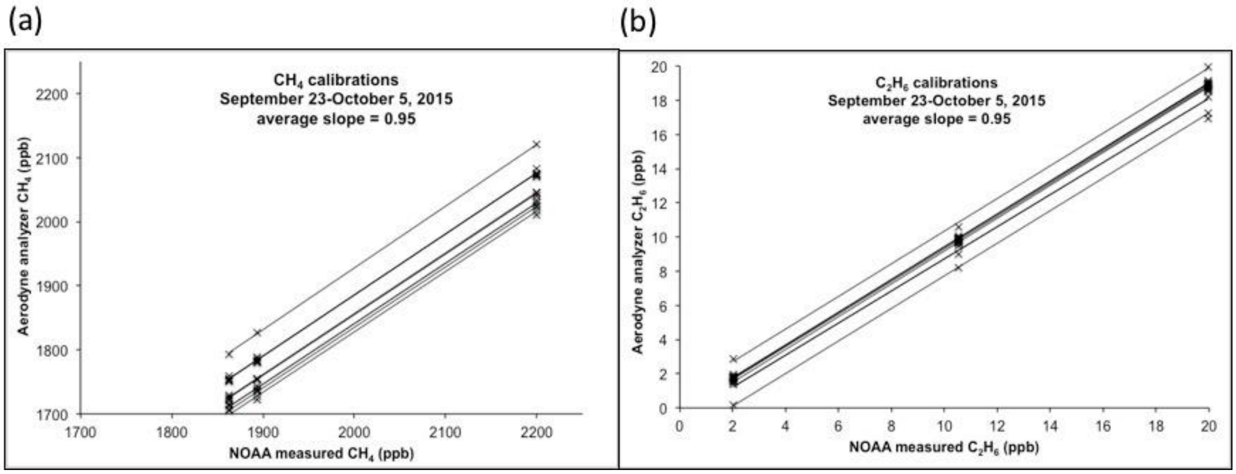


**Figure S1: TILDAs calibration curves**. (a) $CH_4$ calibration curves for September 23-October 5, 2015 (b) $C_2H_6$ calibration curves for September 23-October 5, 2015.

The CRDS was calibrated post-campaign in the NOAA GMD laboratory and correction factors for $CH_4$, $CO_2$ and CO were applied.

## Section 2. Description of mobile laboratory set-up

The mobile laboratory (ML) is an instrumented van with an inlet that extends in front of and above the driver side of the van, ~4 m above the ground. Attached to the inlet is a polytetrafluoroethylene (PTFE) 0.2 μm capsule filter (Whatman, USA). For this field campaign, 1/4" stainless steel tubing connected the filter at the inlet to a "T", where sample air flowed through 1/8" stainless steel tubing to the CRDS, which drew air at ~200 SCCM and through 1/4" stainless steel tubing to the TILDAS, which drew air at ~ 8 SLPM. Regulators of three calibration cylinders were connected with 1/4" stainless steel tubing to a gas manifold comprised of four electronically actuated 3-way valves (Parker, USA). When no valves were actuated, the inlet was connected to vacuum, which flushed ambient air at ~200 SCCM through the calibration line. When a solenoid valve associated with a calibration cylinder was actuated, the vacuum line was closed off, allowing the calibration gas to flow out to the "T" upstream of the instruments and then to the analyzers. Regulators were set so that gas was released with enough pressure to create a ~ 1 L/min overflow at the inlet. An overflow was created to ensure that the calibration gas would be delivered to the instruments with no ambient air. It also allowed the calibration gas to travel the same path as ambient air samples and be delivered to both analyzers simultaneously.

## Section 3. Linearity and saturation of TILDAS instruments

The linear dynamic range of tunable infrared laser direct absorption spectrometer (TILDAS) instruments has been investigated, with results showing linearity over several orders of magnitude, degrading when the absorption line becomes saturated. Experiments were conducted on two different Aerodyne TILDAS instruments: a mini-TILDAS measuring $C_2H_6$ at 2996.85 $cm^{-1}$ with the standard 76 m cell and a dual-TILDAS measuring $CH_4$ (and other unrelated species) at 1294.4 $cm^{-1}$ and equipped with a 204 m cell. The principle of measurement is identical for all TILDAS instruments.

In these experiments, pure $CH_4$ or $C_2H_6$ gas was diluted into ultra-zero air. Flows of pure gases were controlled with an Alicat flow controller and measured with a DryCal flow meter. Zero air flow was set at 23.3 SLPM using a manual valve and the flow also measured with a DryCal flow meter. The TILDAS instruments sub-sampled off of the resulting calibration mixture. Observed concentrations were recorded and compared to the calculated concentration. Results of these experiments are shown in Figure S2 below for $CH_4$ (left) and $C_2H_6$ (right). The maximum linear response level was chosen from the highest calibration point resulting in a linear slope with $R^2$ better than 0.99.

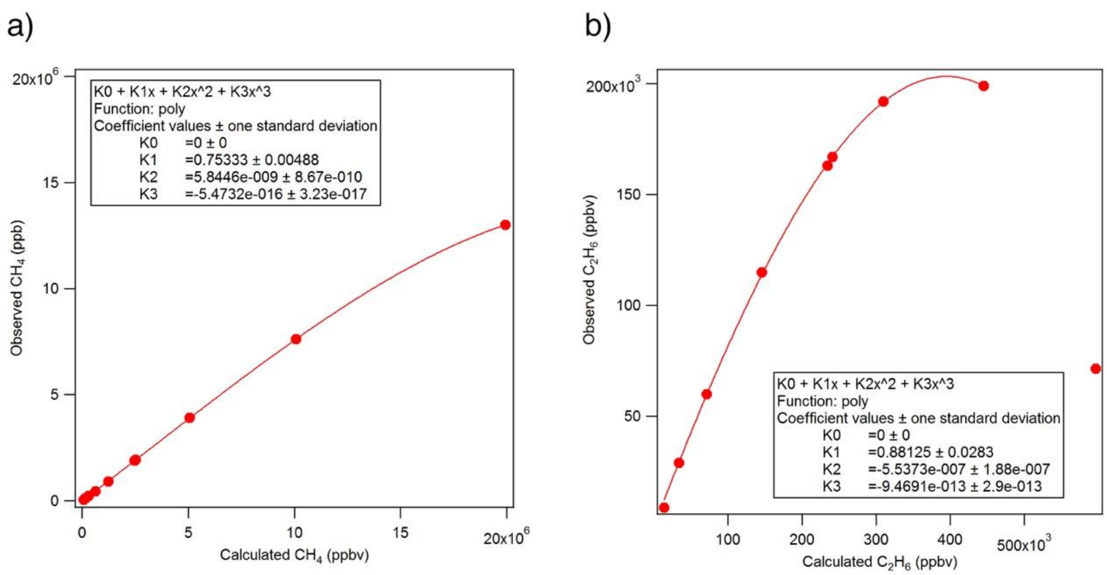


**Figure S2.** Results of linearity and saturation experiments for two TILDAS instruments measuring $CH_4$ (left) and $C_2H_6$ (right).

These two instruments have different absorption linestrengths (and in one case path length) than the mini-TILDAS for $C_2H_6$ and $CH_4$ combined at 2990 $cm^{-1}$, which was used for measurements in the NOAA GMD van. However, all TILDAS instruments rely on Beer's Law, $A = \varepsilon\ c\ \ell$, where $\varepsilon$ is linestrength, $\ell$ is path length, c is concentration, and A is absorbance. The differences in linestrength and path length between instruments are used to calculate an absorbance ratio and estimate the maximum linear response for $C_2H_6$ and $CH_4$ in the 2989-2990 $cm^{-1}$ instrument (Table S2). The NOAA GMD instrument (2989-2990 $cm^{-1}$) is expected to produce a linear $C_2H_6$ measurement over a larger range than the reference instrument, up to ~300 ppm, while the $CH_4$ measurement linearity will only slightly lower, up to ~7200 ppm.

**Table S2.** Measured and estimated maximum linear response levels for selected TILDAS instruments.

| Instrument | Species | Linestrength ε ($cm^2$ $molec.^{-1}$ $cm^{-1}$) | Path length ℓ (m) | Absorbance Ratio (A†/A*) for same concentration | Max Linear Response (ppm) |
|---|---|---|---|---|---|
| mini-TILDAS at 2996.85 $cm^{-1}$ † | $C_2H_6$ | 1.2 E-4 | 76.4 | 2.66 | 115 |
| mini-TILDAS at 2989-2990 $cm^{-1}$ * | $C_2H_6$ | 5.9 E-5 | 76.4 | | ~ 300 |
| dual-TILDAS at 1294.4 $cm^{-1}$ † | $CH_4$ | 1.6 E-1 | 204.3 | 0.96 | 7 620 |
| mini-TILDAS at 2989-2990 $cm^{-1}$ * | $CH_4$ | 5.8 E-2 | 76.4 | | ~ 7 200 |

† reference instruments used for the saturation experiments in Figure S2
* instrument used in the NOAA-GMD van
~ indicates an estimate

## Section 4. Flask measurements of $C_2H_6$ by gas chromatograph mass spectrometry

Flask samples were analyzed for $C_2H_6$ by gas chromatography mass spectrometry (GC-MS) on a custom-built system in the NOAA ESRL GMD laboratory in Boulder, Colorado. This system, known as Perseus (PR1), is used to measure samples collected as part of the Global Greenhouse Gas Reference Network North American Carbon Program and the Halocarbons and other Atmospheric Trace Species (HATS) global remote sampling network. Though only $C_2H_6$ results are used in this work, samples measured by PR1 are analyzed for over 60 halocarbons, hydrocarbons, and sulfur-containing compounds.

When a sample is introduced into the PR1 system, sample air enters a first stage cryogenic trap made of 50 mg divinyl benzene adsorbent (100/120 mesh HayeSep D, Hayes Separations, Banderas, TX) cooled to -165°C, where bulk air constituents that would interfere with analyte analysis are collected in a pre-evacuated, thermostated, fixed-volume reservoir. The difference between the final and initial pressures in this reservoir is used to determine the original sample volume, a value required to ultimately calculate mixing ratios. The reproducibility of pressure measurements is estimated to be 1:10,000.

Once the sample is desorbed at 100°C, it enters a Nafion drying column and next, a second stage cryogenic trap of 5 mg divinyl benzene cooled to -165°C. This second trap of 0.50 mm ID tubing serves to refocus broad peaks and further separate analytes from bulk gases. Following desorption at 100°C, the sample travels to a precolumn, where analytes are separated by molecular weight and the desired lighter, earlier-eluting compounds then enter the main column, a 30m x 0.32 mm GasPro column (Agilent Technologies). Finally, analytes reach the detector, where a mass-to-charge ratio (m/z) of 27 is used to detect $C_2H_6$. Cycle time for one complete analysis is 22.5 minutes.

To track detector drift over time, sets of two to four injections of field samples are bracketed with injections from tanks of whole air 'tertiary' standards. Tests to assess instrument linearity are performed approximately once a week over a range of 10% to 500% of the tertiary gas response by varying for each injection the pressure collected in the reservoir.

Calibration of PR1 field sample results is achieved through a hierarchy of standard gases. The tertiary tanks that are run daily versus field samples as described above are also periodically (every four to six months) compared to a suite of 'secondary' tanks, which are also whole air samples collected in high pressure tanks at Niwot Ridge, Colorado. While a given tertiary may have a service life of about six months before it becomes pressure depleted, the sparing use of secondaries offers the potential for many years of service, allowing all field data to be expressed as relative ratios to one secondary scale, denoted 'S1'. This hierarchy was modeled after that used by the Advanced Global Atmospheric Gases Experiment (Miller et al., 2008).

Absolute calibration of the whole air secondaries is achieved by comparison with synthetic blends, denoted 'primaries'. These are mixtures of pure analyte that are diluted step-wise and gravimetrically with commercial 'zero air', which is an air-like blend of oxygen in nitrogen at approximate atmospheric ratios. The current NOAA 2016 $C_2H_6$ absolute calibration scale is based on repeated comparisons with one such tank, designated ALM067726, which has a gravimetrically-assigned value of 972 ± 2.9 ppt $C_2H_6$. For $C_2H_6$, the largest uncertainty in the primary preparation is the estimated analyte contamination of the diluent gas, which typically contains 1 to 10s of ppt $C_2H_6$. While a total of nine different $C_2H_6$ primaries have been prepared and compared with the secondaries, only results of ALM067726 are used due to a higher confidence in the estimated contamination level. Overall, these comparisons of tertiaries, secondaries and primaries over the past four years have demonstrated stable storage of $C_2H_6$ within most tanks. These periodic comparisons allow any measurable drift within a given tank to be fit with a linear regression and a corresponding correction function estimated and applied.

To estimate the long-term reproducibility of the PR1$C_2H_6$ measurements, one or more tanks from a suite of 50+ 'target tanks' of whole air and gravimetric standards are analyzed weekly. Based on the now four years of all such data, we see no statistically significant drift in our assigned value of the secondary gases for $C_2H_6$. We use the one-sigma standard deviation of all these results to estimate a ±4 ppt reproducibility for $C_2H_6$ for the instrument alone. However, since all the samples involved in this study are acquired and stored in NOAA programmable flask packages (PFPs), long-term (order 30 days) storage tests of known whole air samples in PFPs were performed to assess contamination and storage. Results, which include the instrument uncertainty itself, from testing over 100 PFPs suggests a one-sigma standard deviation of ±11 ppt for the $C_2H_6$ data presented here.


References:

Miller, B. R., Weiss, R. F., Salameh, P. K., Tanhua, T., Greally, B. R., Mühle, J. and Simmonds, P. G., Medusa: A sample preconcentration and GC/MS detector system for in situ measurements of atmospheric trace halocarbons, hydrocarbons and sulfur compounds, *Anal. Chem.*, 80, 1536-1545, 10.1021/ac702084k, 2008.


## Section 5. Flight patterns

Flights were conducted in either a box pattern or raster pattern to gather data for a mass balance $CH_4$ flux calculation or to map the variety of emission source plumes in the study area, respectively. Two examples are shown below.

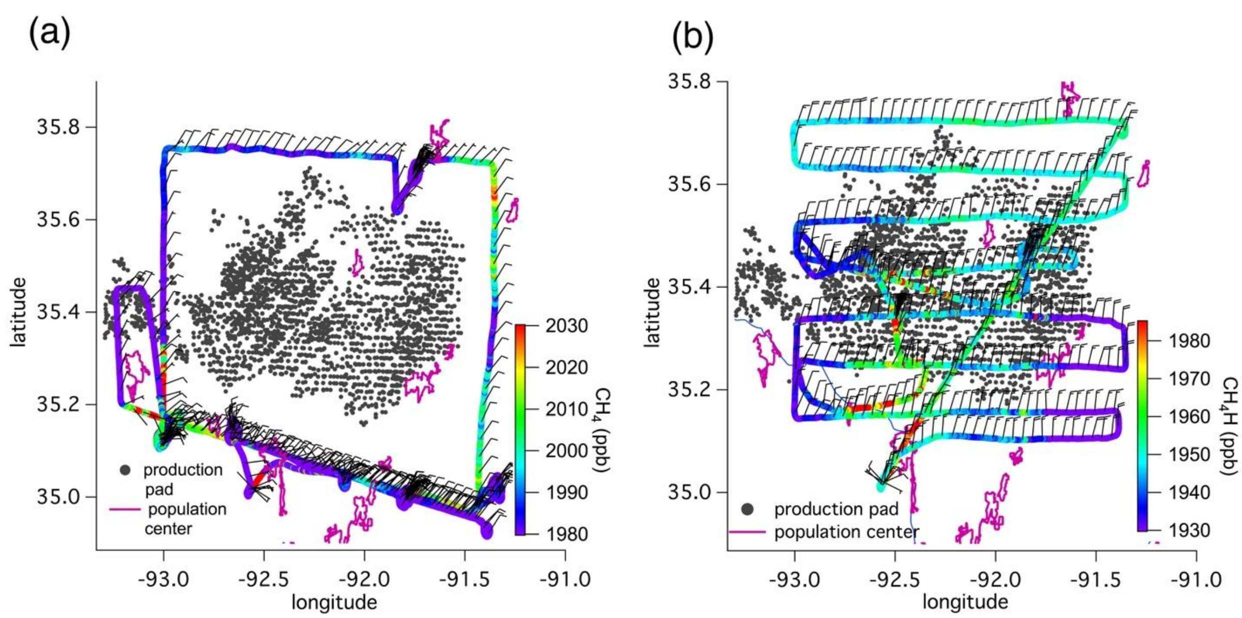


**Figure S3: Examples of flight patterns conducted during campaign.** (a) A box flight pattern around the study area on September 26, 2015 (b) a raster pattern over the study area on October 2, 2015.

## Section 6. Determination of $C_2H_6$ to $CH_4$ enhancement ratios using mobile lab in situ data

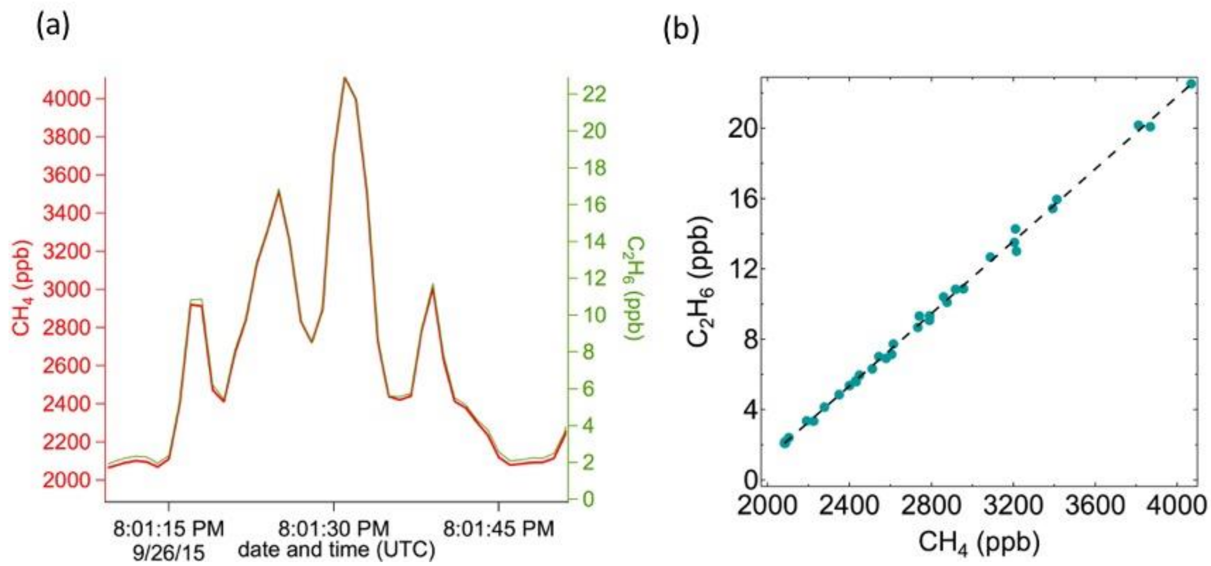


**Figure S4**: **Example of ER determination from ML measurements.** (A) Example of in situ $CH_4$ (red) and $C_2H_6$ (green) measurements downwind of a production pad. (B) The resulting $C_2H_6$ vs. $CH_4$ plot for the facility, which gives a slope determined by least squares regression of 1.0% and an $R^2$ of 0.99.

## Section 7. ERs for a production pad with evidence of combustion

**Table S3: ERs from a production pad where correlation of $CH_4$ and $CO_2$ was observed.** In situ $C_2H_6$ to $CH_4$ and $CO_2$ to $CH_4$ ERs from all $CH_4$ plumes measured at one production pad at which combustion likely occurred during a portion of the measurements. $CO_2$ and $CH_4$ data used to calculate $CO_2$ to $CH_4$ ERs are from the CRDS.

| date | plume duration (seconds) | $CH_4$ enhancement (ppb) | $C_2H_6$ to $CH_4$ ER | $R^2$ | $CO_2$ to $CH_4$ ER (ppm/ppb) | $R^2$ |
|---|---|---|---|---|---|---|
| 9/24/2015 | 24 | 521 | 0.9% | 0.99 | 0.01 | 0.77 |
| 9/24/2015 | 143 | 324 | 0.9% | 0.99 | no correlation | N/A |
| 9/24/2015 | 63 | 98 | 0.8% | 0.97 | 0.09 | 0.66 |
| 9/24/2015 | 129 | 472 | 0.9% | 0.99 | 0.01 | 0.48 |
| 9/24/2015 | 57 | 51 | 11.6% | 0.97 | 2.04 | 0.91 |
| 9/24/2015 | 9 | 38 | 5.3% | 0.99 | 2.80 | 0.97 |
| 9/24/2015 | 13 | 38 | 5.9% | 0.99 | 2.50 | 0.99 |
| 9/24/2015 | 43 | 199 | 1.0% | 0.92 | 0.02 | 0.49 |
| 9/28/2015 | 59 | 292 | 0.9% | 0.99 | 0.01 | 0.99 |
| 9/28/2015 | 57 | 224 | 0.9% | 0.98 | 0.01 | 0.98 |
| 9/28/2015 | 22 | 150 | 0.9% | 0.99 | 0.01 | 0.99 |
| 9/28/2015 | 47 | 240 | 0.9% | 0.97 | 0.01 | 0.97 |
| 9/28/2015 | 45 | 81 | 1.0% | 0.86 | 0.01 | 0.86 |
| 9/28/2015 | 93 | 707 | 0.9% | 1.00 | 0.01 | 1.00 |
| 10/2/2015 | 63 | 538 | 0.9% | 0.98 | no correlation | N/A |

## Section 8. $C_2H_6$ to $CH_4$ ERs determined by aircraft spirals

The aircraft flew in a spiral pattern around potential $CH_4$ sources and these data were used to calculate ERs at each location. "N/A" indicates that an ER could not be determined due to low or no correlation between $C_2H_6$ and $CH_4$.

**Table S4: Facility-level ERs determined from aircraft.** List of the type of NG and non-NG facilities and locations at which aircraft data were used to determine an ER.

| Type of $CH_4$ source | Flight date and mean time (UTC) | $C_2H_6$ to $CH_4$ ER |
|---|---|---|
| Production pads | 9/24/2015 18:42 | 2.5% |
| Production pads | 10/3/2015 20:06 | 2.1% |
| Production pads | 10/14/2015 19:48 | 1.5% |
| Production pads | 10/14/2015 20:24 | 1.6% |
| Production pads | 10/7/2015 17:12 | 1.5% |
| Gathering station | 9/24/2015 17:00 | 2.1% |
| Gathering station | 9/30/2015 18:30 | 1.4% |
| Gathering station | 10/2/2015 19:18 | 1-2% |
| | 10/3/2015 19:48 | 1% |
| Gathering station | 10/3/2015 18:48 | N/A |
| Gathering station | 10/3/2015 20:30 | 1.9% |

| | | |
|---|---|---|
| Gathering station and nearby production pads | 10/3/2015 19:24 | 1.9% |
| Gathering station | 10/5/2015 20:18 | N/A |
| Gathering station | 10/6/2015 20:42 | 2.2% |
| Gathering station | 10/7/2015 21:18 | 0.9% |
| Transmission station | 9/23/2015 17:18 | 2.5% |
| Poultry farm | 9/23/2015 19:00 | N/A |
| | 9/24/2015 17:30 | N/A |
| Landfill | 9/25/2015 20:24 | N/A |
| | 10/13/2015 21:18 | N/A |
| Landfill | 10/13/2015 16:36 | N/A |
| Landfill | 10/13/2015 20:06 | N/A |
| Landfill | 10/13/2015 20:36 | N/A |
| Landfill | 10/13/2015 20:54 | N/A |
| Biomass burning | 9/30/2015 17:48 | 7.7% |
| Biomass burning | 10/1/2015 17:30 | 6.3% |
| Water treatment plant | 10/6/2015 15:54 | N/A |

## Section 9. Poultry farm measurements

**Table S5: Poultry farm measurement locations.** Locations of the operating poultry farms measured by the mobile laboratory. Substantial $CH_4$ enhancements were not identified downwind of any of these poultry farms.

| latitude | longitude |
|---|---|
| 35.3175° | -92.8837° |
| 35.3663° | -92.7165° |
| 35.4384° | -92.5190° |
| 35.4073° | -92.6917° |
| 35.3266° | -92.7067° |
| 35.3030° | -92.7214° |
| 35.6547° | -91.9145° |
| 35.4782° | -91.7971° |
| 35.3247° | -92.6964° |

## Section 10. Delaunay Triangulation Method

A Delaunay Triangulation algorithm in MATLAB was used to connect NG facilities at which ERs were determined into triangles and weight the ERs by the total NG production at production pads within those triangles. A production-weighted average ER was then obtained for the whole study area and each half.

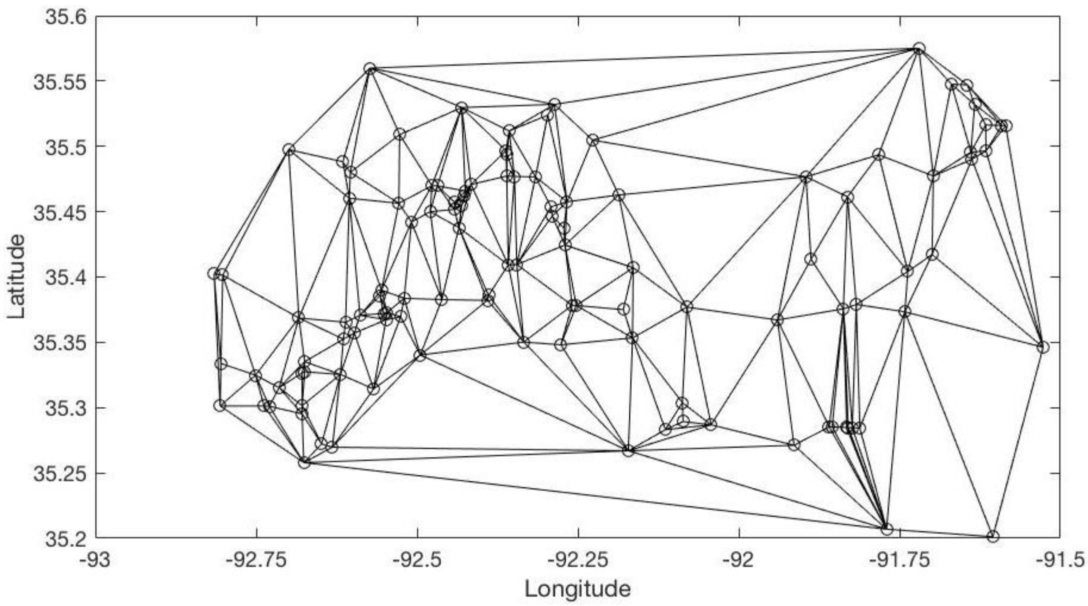


**Figure S5: Delaunay Triangulation.** An illustration of the Delaunay Triangulation algorithm used to connect the 114 facilities at which ERs were determined from mobile laboratory data. Each open circle is a facility at which an ER was obtained from ML measurements.

## Section 11. Area-scale $C_2H_6$ to $CH_4$ ERs from each flight transect or leg

**Table S6: Description of flights.** List of all flights conducted over the study area from September 21 to October 14, 2015 and the rationale for inclusion in or exclusion from ER calculations

| Date | Flight pattern/target | Used for determination of area-scale ER? |
|---|---|---|
| September 21, 2015 | box pattern, no mass balance | No. Wind speed was too low to have transported emissions downwind at time of measurements. |
| September 22, 2015 | raster over entire study area | Yes. One leg used to determine an area-scale ER of 1.2 ± 0.03% for the western half of the study area. |
| September 23, | box pattern, no mass balance | No. Downwind transects each had one of the |

| | | |
|---|---|---|
| 2015 | | following issues: unknown TILDAS problem, $C_2H_6$ and $CH_4$ signals that were too low relative to instrument noise, or too high of an altitude relative to other downwind transects. |
| September 24, 2015 | raster over Clebourne County and site-level measurements within the county | No. Flight pattern not appropriate for determining area-scale ERs. |
| September 25, 2015 | raster over Conway and Faulkner counties to examine poultry farms | No. Flight pattern not appropriate for determining area-scale ERs. |
| September 26, 2015 | box pattern, no mass balance | No. Downwind transects were not conducted at the same altitude each time, making direct comparison of the results of each impossible. |
| September 30, 2015 | aborted flight | No. Not used due to cloud cover that day. |
| October 1, 2015 | successful study area mass balance | No. $C_2H_6$ signal was too low relative to instrument noise due to high wind speeds, which dispersed plumes. |
| October 2, 2015 | successful study area mass balance | Yes. One leg used to determine an area-scale ER of 1.1 ± 0.04% for the western half of the study area. |
| October 3, 2015 | Tracer release test and site-level measurements | No. Flight pattern not appropriate for determining area-scale ERs. |
| October 5, 2015 | raster over the western half of the study area | Yes. Seven legs used to determine an area-scale ER of 1.2 ± 0.03% for the western half of the study area. |
| October 6, 2015 | raster over the eastern half of the study area | Yes. Four legs used to determine an area-scale ER of 1.3 ± 0.05% for the western half of the study area. |
| October 7, 2015 | raster over the western half of the study area | Yes. Ten legs used to determine an area-scale ER of 1.3 ± 0.04% for the western half of the study area. |
| October 13, 2015 | city of Little Rock mass balance | No. Flight pattern not appropriate for determining area-scale ERs. |

| | | |
|---|---|---|
| October 14, 2015 | raster over the eastern half of the study area | No. This was a raster flight over the eastern half of the study area and cannot be used for attribution because the bimodal distribution of NG ERs in the East makes attribution using the model proposed in this paper impossible. |

**Table S7: Description of legs or transects in flights used for attribution.** For flights that were used for the determination of an area-scale ER for the western half, all legs or transects are listed and described.

| Date | Transect or leg | time (UTC) | ER | uncertainty | $R^2$ | number of data points | used for determination of area-scale ER? |
|---|---|---|---|---|---|---|---|
| September 22, 2015 | Downwind 1 | 16:29-16:41 | N/A | N/A | N/A | 134 | No. Transect was conducted too early to ensure planetary boundary layer was well-mixed. |
| | 1 | 16:46-17:00 | N/A | N/A | N/A | 202 | No. Transect was conducted too early to ensure planetary boundary layer was well-mixed. |
| | 2 | 17:07-17:17 | N/A | N/A | N/A | 177 | No. Transect was conducted too early to ensure planetary boundary layer was well-mixed. |
| | 3 | 17:20-17:34 | N/A | N/A | N/A | 251 | No. Transect was conducted too early to ensure planetary boundary layer was well-mixed. |
| | 4 | 17:36-17:51 | N/A | N/A | N/A | N/A | Data not recorded during this leg. |
| | 5 | 17:53-18:07 | N/A | N/A | N/A | 305 | No. Localized $CH_4$ enhancement. |
| | 6 | 18:10-18:24 | N/A | N/A | N/A | 304 | No. $C_2H_6$ enhancements < 1 ppb and $CH_4$ enhancements < 50 ppb |
| | 7 | 18:28 - 18:32 | N/A | N/A | N/A | 96 | No. Upwind leg. |
| | 8 | 18:43-18:58 | N/A | N/A | N/A | 303 | No. Upwind leg. |
| | 9 | 19:01-19:14 | N/A | N/A | N/A | 299 | No. Upwind leg. |
| | 10 | 19:17-19:32 | N/A | N/A | N/A | 308 | No. Upwind leg. |

| | | | | | | | |
|---|---|---|---|---|---|---|---|
| | 11 | 19:34-19:48 | N/A | N/A | N/A | 293 | No. Upwind leg. |
| | 12 | 19:50-20:05 | N/A | N/A | N/A | 313 | No. Upwind leg. |
| | 13 | 20:08-20:22 | N/A | N/A | N/A | 309 | No. Upwind leg. |
| | Downwind 2 | 20:56-21:12 | 1.20% | 0.03% | 0.69 | 317 | Yes. |
| | Downwind 3 | 21:15-21:54 | | | | N/A | No. Unknown TILDAS problem. |
| October 2, 2015 | 1 | 16:07-16:38 | N/A | N/A | N/A | 948 | No. Upwind leg. |
| | 2 | 16:40-17:11 | N/A | N/A | N/A | 965 | No. Upwind leg. |
| | 3 | 17:13-17:44 | N/A | N/A | N/A | 909 | No. $C_2H_6$ enhancements < 1 ppb and $CH_4$ enhancements < 50 ppb |
| | 4 | 17:47-18:13 | 1.08% | 0.04% | 0.64 | 305 | Yes. |
| | 5 | 19:47-20:19 | N/A | N/A | N/A | 942 | No. $C_2H_6$ enhancements < 1 ppb and $CH_4$ enhancements < 50 ppb |
| | 6 | 20:22-20:53 | N/A | N/A | N/A | 969 | No. $C_2H_6$ enhancements < 1 ppb and $CH_4$ enhancements < 50 ppb |
| | 7 | 20:58 - 21:31 | N/A | N/A | N/A | 903 | No. $C_2H_6$ enhancements < 1 ppb and $CH_4$ enhancements < 50 ppb |
| October 5, 2015 | 1 | 16:14-16:30 | N/A | N/A | N/A | 316 | No. Upwind leg. |
| | 2 | 16:33-16:45 | N/A | N/A | N/A | 226 | No. Upwind leg. |
| | 3 | 16:46-17:04 | N/A | N/A | N/A | 342 | No, $CH_4$ enhancements < 50 ppb. |
| | 4 | 17:05-17:21 | 1.30% | 0.03% | 0.77 | 63 | Yes. |
| | 5 | 17:22-17:38 | 1.29% | 0.03% | 0.89 | 200 | Yes. |
| | 6 | 17:39-17:54 | 1.33% | 0.03% | 0.85 | 180 | Yes. |

| | | | | | | | |
|---|---|---|---|---|---|---|---|
| | 7 | 17:56-18:12 | 1.05% | 0.04% | 0.84 | 116 | Yes. |
| | 8 | 18:13-18:29 | 1.07% | 0.04% | 0.85 | 97 | Yes. |
| | 9 | 18:30-18:47 | 1.15% | 0.03% | 0.91 | 142 | Yes. |
| | 10 | 18:48-19:04 | 1.22% | 0.05% | 0.67 | 215 | Yes. |
| | 11 | 19:05-19:17 | N/A | N/A | N/A | 244 | No. $R^2$ below threshold. |
| | 12 | 19:21-19:37 | N/A | N/A | N/A | 198 | No. $R^2$ below threshold. |
| | 13 | 19:38-19:52 | N/A | N/A | N/A | 288 | No. $R^2$ below threshold. |
| October 6, 2015 | 1 | 16:04-16:19 | 1.39% | 0.04% | 0.91 | 143 | Yes. |
| | 2 | 16:20-16:35 | 1.38% | 0.04% | 0.88 | 157 | Yes. |
| | 3 | 16:36-16:52 | 1.35% | 0.05% | 0.82 | 188 | Yes. |
| | 4 | 16:54-17:09 | 1.13% | 0.06% | 0.65 | 181 | Yes. |
| | 5 | 17:10-17:28 | 1.31% | 0.06% | 0.64 | 213 | No. $C_2H_6$ enhancements < 1 ppb. |
| | 6 | 17:30-17:47 | N/A | N/A | N/A | 341 | No. $C_2H_6$ enhancements < 1 ppb. |
| | 7 | 17:49-18:07 | N/A | N/A | N/A | 364 | No. $C_2H_6$ enhancements < 1 ppb. |
| | 8 | 18:09-18:26 | N/A | N/A | N/A | 336 | No. Measurements appear to be of two distinct sources rather than a mix. |
| | 9 | 18:28-18:46 | N/A | N/A | N/A | 356 | No. Measurements appear to be of two distinct sources rather than a mix. |
| | 10 | 18:48-19:05 | N/A | N/A | 0.20 | 201 | $CH_4$ enhancements < 50 ppb |
| | 11 | 19:06-19:25 | N/A | N/A | 0.42 | 254 | $C_2H_6$ enhancements < 1 ppb and CH4 enhancements < 50 ppb |

| | | | | | | | |
|---|---|---|---|---|---|---|---|
| | 12 | 19:26-19:44 | N/A | N/A | 0.37 | 182 | $C_2H_6$ enhancements < 1 ppb and CH4 enhancements < 50 ppb |
| | 13 | 19:38 - 19:55 | 1.61% | 0.01% | 0.57 | 276 | $C_2H_6$ enhancements < 1 ppb and $CH_4$ enhancements < 50 ppb |
| October 7, 2015 | 1 | 16:08-16:19 | N/A | N/A | 0.59 | 213 | No. $C_2H_6$ enhancements < 1 ppb |
| | 2 | 16:20-16:32 | N/A | N/A | 0.51 | 221 | No. $C_2H_6$ enhancements < 1 ppb |
| | 3 | 17:41 – 17:53 | 1.31% | 0.03% | 0.80 | 219 | Yes. |
| | 4 | 17:54-18:07 | 1.28% | 0.03% | 0.83 | 232 | Yes. |
| | 5 | 18:08-18:22 | 1.28% | 0.02% | 0.90 | 259 | Yes. |
| | 6 | 18:23-18:37 | 1.33% | 0.03% | 0.83 | 253 | Yes. |
| | 7 | 18:38-18:52 | 1.30% | 0.03% | 0.83 | 256 | Yes. |
| | 8 | 18:53-19:07 | 1.07% | 0.05% | 0.73 | 201 | Yes. |
| | 9 | 19:08-19:21 | 1.18% | 0.04% | 0.85 | 194 | Yes. |
| | 10 | 19:22-19:36 | 1.36% | 0.06% | 0.69 | 219 | Yes. |
| | 11 | 19:38-19:51 | N/A | N/A | 0.40 | 254 | No. $C_2H_6$ enhancements < 1 ppb |
| | 12 | 19:52-20:06 | 1.42% | 0.07% | 0.76 | 153 | Yes. |
| | 13 | 20:07-20:19 | 1.32% | 0.05% | 0.67 | 357 | Yes. |
| | 14 | 20:20 – 20:30 | N/A | N/A | N/A | 191 | No. Different spatial coverage of study area than legs 1-13. |
| | 15 | 20:31-20:39 | N/A | N/A | N/A | 158 | No. Different spatial coverage of study area than legs 1-13. |
| | 16 | 20:40 – 20:49 | N/A | N/A | N/A | 165 | No. Different spatial coverage of study area than legs 1-13. |

## Section 12. Comparison of in situ $C_2H_6$ to $CH_4$ enhancement ratios with discrete flask samples

**Figure S6** compares the ERs derived for two well pads and three gathering stations based on in situ and discrete flask air sample $CH_4$ and $C_2H_6$ measurements. Measurement periods for these facility plumes range from one minute to one hour and include in situ measurements made both when the ML was stationary and mobile. ERs from flask air are calculated using only samples collected during the same day and within ~30 minutes, permitting the assumption that the background (to which all $CH_4$ and $C_2H_6$ enhancements are relative) is the same for all samples collected at the same location.

ERs determined from ML in situ data show strong agreement with those calculated using results from flask air sample analysis. This demonstrates the usefulness of fast response in situ measurements for obtaining a large number of ER data points throughout the study area in order to obtain representative statistics for the NG infrastructure. Discrepancies, the largest of which is 17% (production pad with a 1.1% in situ multiple plume time-weighted average ER and 1.3% flask ER), are expected because flask air sampling often gives one 20 to 30 sec "snapshot" (flask fill time) while the ER from in situ data is usually a time-weighted average of ERs from multiple plumes from the same facility. The variability in minimum and maximum observed in situ ERs (shown by error bars in **Figure S6**) explains the small disagreement observed between the time-weighted average in situ ER and the flask air sample ER. The one facility (production pad) with the most variability in ER deviates farthest from the 1:1 line while facilities with no variability in in situ ER are along the 1:1 line.

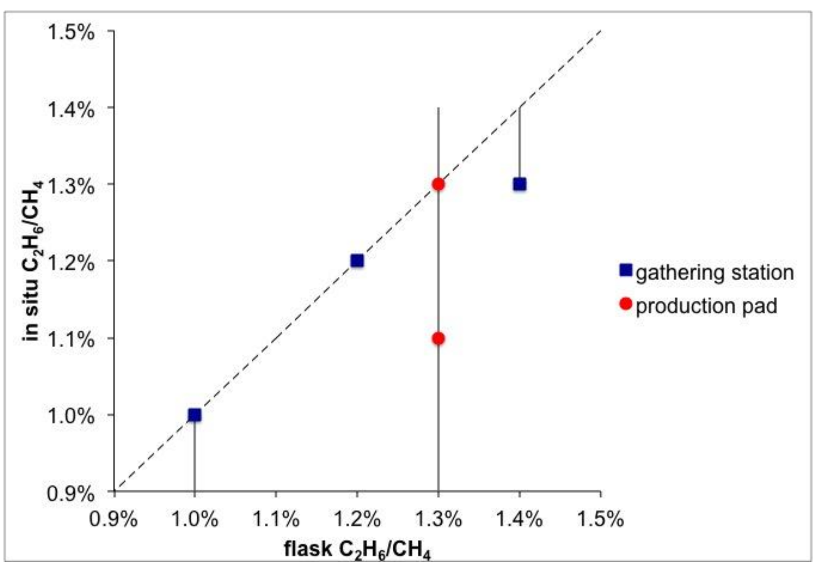


**Figure S6: In situ ERs compared with flask air ERs**. Comparison of $C_2H_6$ to $CH_4$ ERs results for emission plumes from five NG facilities at which three or more discrete flask samples were collected. The vertical error bars indicate the full range of in situ ERs observed from multiple plumes downwind of the same facility over the course of one or two measurement days. The dashed line indicates the 1:1 line.